



Calcined oil sands fine tailings as a supplementary cementing material for concrete

R.C.K. Wong^{a,*}, J.E. Gillott^a, S. Law^a, M.J. Thomas^a, C.S. Poon^b

^aDepartment of Civil Engineering, The University of Calgary, 2500 University Drive NW, Calgary, Alberta, Canada T2N 1N4

^bDepartment of Civil and Structural Engineering, The Hong Kong Polytechnic University, Hong Kong, China

Received 12 December 2002; accepted 12 December 2003

Abstract

In recent years, metakaolin (MK) has received considerable attention, as a high-performance pozzolanic supplementary cementing material for use in concrete. MK is produced by calcining kaolinite at temperatures between 600 and 1000 °C. In the province of Alberta, Canada, the oil sand mining industry produces millions of cubic metres of oil sand tailings that could become a major source of MK. This paper summarizes the behaviour of calcined fine tailings (CFT) as a supplementary cementing material in high-performance concrete and compares its performance to that of MK and silica fume (SF). It was found that CFT has excellent pozzolanic activity in concrete, making it an environmentally friendly and potentially cost effective supplement.

© 2003 Elsevier Ltd. All rights reserved.

Keywords: Metakaolin; Calcined oil sand fine tailings; Silica fume; Concrete; Cement

1. Introduction

In the province of Alberta, Canada, the oil sands mining industry produces large volumes of tailings. The tailings (coarse and fine) are pumped to the tailing management area, where the sand settles quickly, and a suspension of silt and clay flows into the tailings settling area in huge engineered earth-structure dams (Morgenstern et al. [1]). In this disposal method, the fine tailings are treated as a waste product of no value and impose a major environmental challenge to the region. Environmental concerns have driven oil producers to seek solutions for more effective disposal methods or alternate usage of the tailings. At the two existing oil producers, Suncor and Syncrude, there is currently over 400 Mm³ of fine tailings containing some 60 M tons of kaolin.

Recently, there has been much research into the use of metakaolin (MK) as a pozzolan supplement for concrete mixes [2–7]. MK is produced from pure kaolinite by high-temperature calcination. Mostly, these re-

search efforts have focused on MK's ability to remove calcium hydroxide (CH) from the cement, as CH is associated with poor durability. Replacement of calcium hydroxide with calcium silicate hydrate (C–S–H) gel not only improves resistance to sulfate attack and alkali–silica reaction (ASR), but also provides enhanced strength, which is derived from the additional cementitious phases generated by the reaction of calcium hydroxide with MK.

Raw oil sands fine tailings are largely made up of kaolinite and some other clay minerals including illite and smectite. High-temperature calcination converts the kaolinite into pozzolanic products, principally MK, which can be used as a supplementary cementing material in concrete. This paper investigates the potential use of calcined fine tailings (CFT) as a supplementary cementing material in concrete. A series of tests were conducted on the properties of freshly mixed and hardened concrete specimens containing CFT. The results were compared with those obtained from other concrete mixes containing commercially available pozzolan supplements, that is, silica fume (SF) and MK. In addition, the pozzolanic and alkali–silica reaction properties of SF, MK, and CFT in blended cement pastes and mortar bars were compared.

* Corresponding author. Tel.: +1-403-220-4998; fax: +1-403-282-7026.

E-mail address: rckwong@ucalgary.ca (R.C.K. Wong).

2. Experimental program

2.1. Concrete mixes—materials and testing procedures

Three types of supplementary cementing pozzolans were used in this study: SF, MK, and calcined oil sands fine tailings (CFT). SF and MK were supplied from a local concrete producer, and CFT was produced by calcining the raw fine tailings at 700 °C with grinding in a local China factory. Chemical and physical properties of these materials are given in Table 1, along with those of Portland cement (PC).

The concrete mix proportions are given in Table 2. The control mix contained only CSA Type 10 (ASTM type I) cement as the cementing material. In the other three mixes, 7.5% of cement was replaced by an equal quantity of SF, MK, and CFT. The water-to-binder ratio (w/b) for all four mixes was maintained at 0.34. All concrete mixes were prepared using a mechanical mixer. Each mix batch had a yield of 0.1 m³. Tests on the properties of freshly mixed concrete included the following: slump (ASTM C39), unit weight (ASTM C138), and air content ASTM (C231). All tests on the properties of freshly mixed concrete were conducted immediately after the mixing.

Concrete specimens were cast in cylinder or rectangular beam molds using an external vibration table. After the casting, the molds were covered with a plastic sheet. All hardened specimens were removed from the molds in 24 h, and were cured inside a fog room. Tests on the properties of hardened concrete included the following: compressive strength (ASTM C39), flexural strength (ASTM C78), length change of hardened concrete (ASTM C157), static modulus of elasticity (ASTM C469), resistance of concrete to rapid freezing and thawing (ASTM C666), scaling resistance of concrete surfaces exposed to deicing chemicals (ASTM C672), and rapid chloride permeability (ASTM C1202). The curing period varied with each test. For compressive strength tests, cylindrical specimens (102 × 203 mm or 4 × 8 in.) were cast and cured for

Table 1
Chemical and physical properties of Portland cement (PC), silica fume (SF), metakaolin (MK), and calcined oil sands tailings (CFT)

Mass percentage (%)				
Content	Portland cement	Silica fume	Metakaolin	Calcined fine tailings
SiO ₂	20.8	96.0	53.2	54–57
Al ₂ O ₃	4.4	0.3	43.9	30–34
Fe ₂ O ₃	1.5	0.2	0.4	3–4
CaO	63.5	0.3	0.02	0.2–0.5
MgO	4.3	0.5	0.05	1.2–1.4
K ₂ O	0.3	0.4	0.1	2.5–3.0
Na ₂ O	0.4	0.3	0.2	—
SO ₃	2.4	—	—	—
LOI	0.9	0.2	0.5	1.1–1.5
Specific gravity	3.14	2.22	2.61	2.62
Specific surface area (m ² /g)	3.5	19.8	9.8	24.0

Table 2

Concrete mix proportions

Material	Quantities (kg/m ³)
Cementitious material	450
Water	152
Water/binder ratio	0.34
Sand	152
Coarse aggregates (14 mm)	740
Air entrainer (Matersbuilder)	1.4 ml/kg of cementitious material
Superplasticizer (Rheobuild 1000)	15.8 ml/kg of cementitious material

periods of 3, 7, 14, 28, and 90 days. For flexural strength and scaling resistance tests, rectangular beam specimens of 102 × 102 × 356 mm (4 × 4 × 14 in.) and slabs of 305 × 305 × 75 mm (12 × 12 × 3 in.) were prepared and cured for 28 days. For rapid freezing–thawing tests, rectangular beam specimens of 76 × 76 × 279 mm (3 × 3 × 11 in.) were prepared, and cured for 14 days. For rapid chloride permeability tests, cylinder concrete cores of 102 mm in diameter × 51 mm in length (4 × 2 in.) were cut from the concrete cylindrical specimens (102 × 203 mm or 4 × 8 in.) that had been cured for 28 days. For length changes tests, rectangular beam specimens of 76 × 76 × 279 mm (3 × 3 × 11 in.) were moist and air cured for 28 days. For repeatability purposes, three specimens were prepared and tested for each test set. The average values of three test specimens were reported.

2.2. Blended cement pastes—materials and testing procedures

Plain PC pastes without any pozzolan replacement were prepared as the control. Three other blended cement pastes were prepared with three supplementary cementing materials (SF, MK, and CFT) of 7.5% replacement. The water-to-binder ratio (w/b) for all the pastes was 0.34. The paste specimens were mixed in a mechanical mixer. Small amounts of superplasticizer were added to achieve proper consistency. Cube specimens of 50 × 50 × 50 mm (2 × 2 × 2 in.) were cast in steel molds, and covered with a plastic sheet. They were removed from the molds after 1 day, and were then cured in the fog room.

At designated periods of time (3, 7, 14, and 28 days), the cement paste specimens were removed from the fog room, broken into small pieces, and put in an oven at 105 °C for 24 h. This heating allowed all water to vaporize and stop the hydration. These dried and broken pieces were ground to pass a 150-μm sieve for the determination of the pore size distribution and porosity and the Ca(OH)₂ content of the blended cement pastes.

The pore size distribution of the paste specimens were determined using a “Quanta Chrome Autoscan 60” mercury intrusion porosimeter (MIP) with a maximum mercury intrusion pressure of 517 MPa. Cylindrical pore geometry and a contact angle θ of 140° were assumed [8,9]. The mercury intruded pore diameter d_p at an intrusion pressure

of P_{In} was calculated from $d_p = -4\gamma\cos\theta/P_{In}$, where $\gamma = 0.483 \text{ MNm}^{-1}$, the surface tension of mercury [8].

The Ca(OH)_2 content was determined using a “DuPont Instruments 951” thermogravimetric analyser. A quantity of 100 mg of ground sample was heated at the rate of $10^\circ\text{C}/\text{min}$ in nitrogen gas at atmospheric pressure. The Ca(OH)_2 compound was decomposed into CaO and H_2O components, and the H_2O was vaporized during the combustion of Ca(OH)_2 between 425 and 550°C . Thus, the mass of Ca(OH)_2 was given as the mass of H_2O lost in combustion multiplied by the molecular weight ratio of Ca(OH)_2 to H_2O (i.e., $74.01/18.02$), and expressed as percentages by the mass of the original cement content in the sample.

2.3. Mortar bars—materials and testing procedures

Mortar bars containing a highly reactive aggregate (Pyrex-Borosilicate glass), were prepared and tested to compare

the effectiveness of SF, MK, and CFT in preventing excessive expansion of concrete due to the alkali–silica reaction (ASR). The materials used and testing procedures were in accordance with ASTM C441.

The mortar mix proportions for the control mix were 400 g of a high-alkali cement and 900 g of Pyrex glass aggregate. The high-alkali cement contained approximately 1.0% total alkalis, as sodium oxide (Na_2O) plus 0.658% potassium oxide (K_2O). The Pyrex glass aggregate was made from solid glass rods crushed, sieved, cleaned, dried, and graded according to the specifications of ASTM C441. Four different test mixes were prepared. The first test mix contained only Portland cement (CSA Type 10) as the cementing material. In the other three mixes, 7.5% of Portland cement was replaced by an equal quantity of SF, MK, and CFT. The water-to-binder ratio (w/b) for all mortar mixes was 0.34. All mixes were prepared using a mechanical mixer. Mortar bar specimens were cast in rectangular

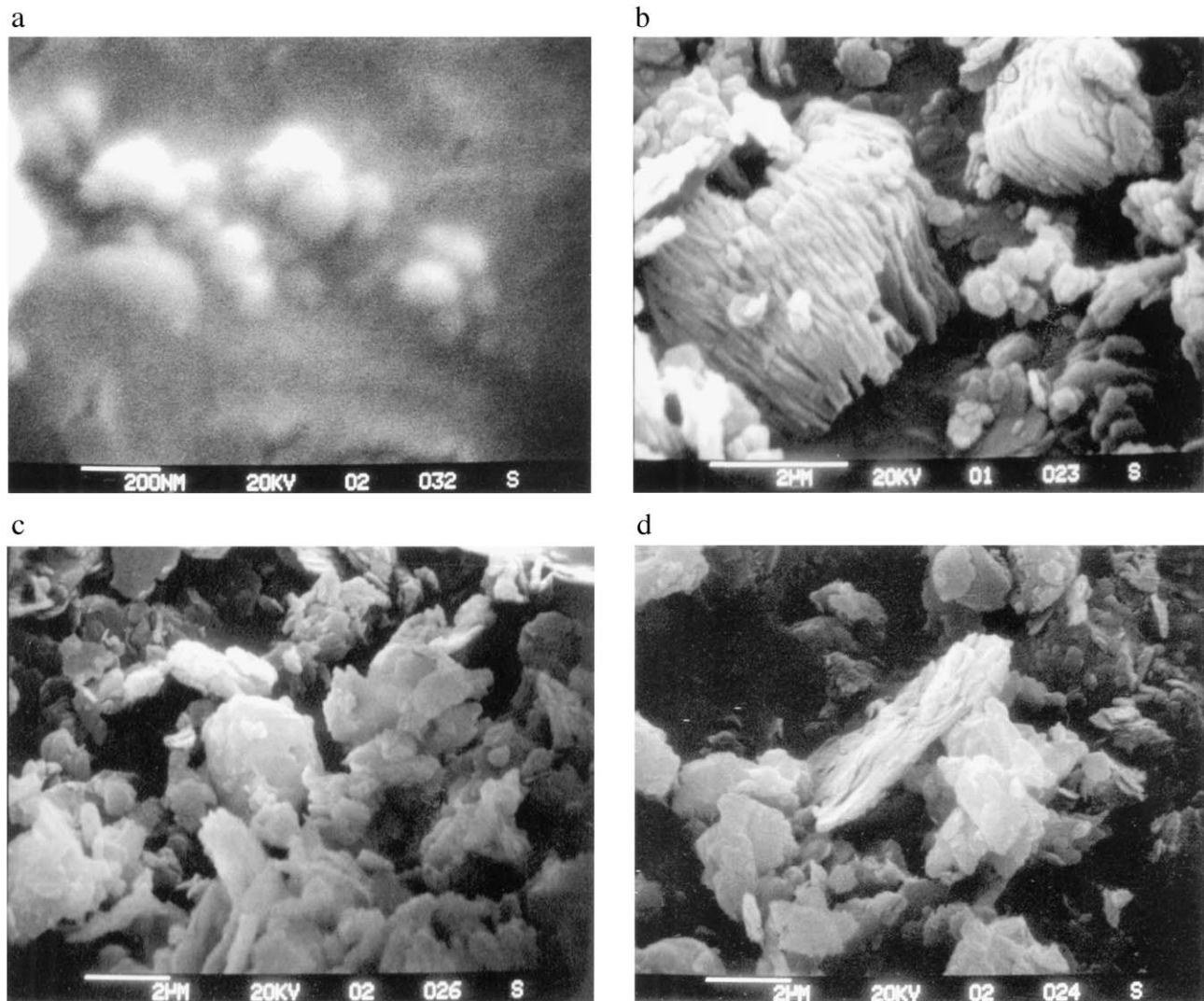


Fig. 1. (a) SEM photo of silica fume (SF). (b) SEM photo of metakaolin (MK). (c) SEM photo of calcined oil sands fine tailings (CFT). (d) SEM photo of illites in CFT.

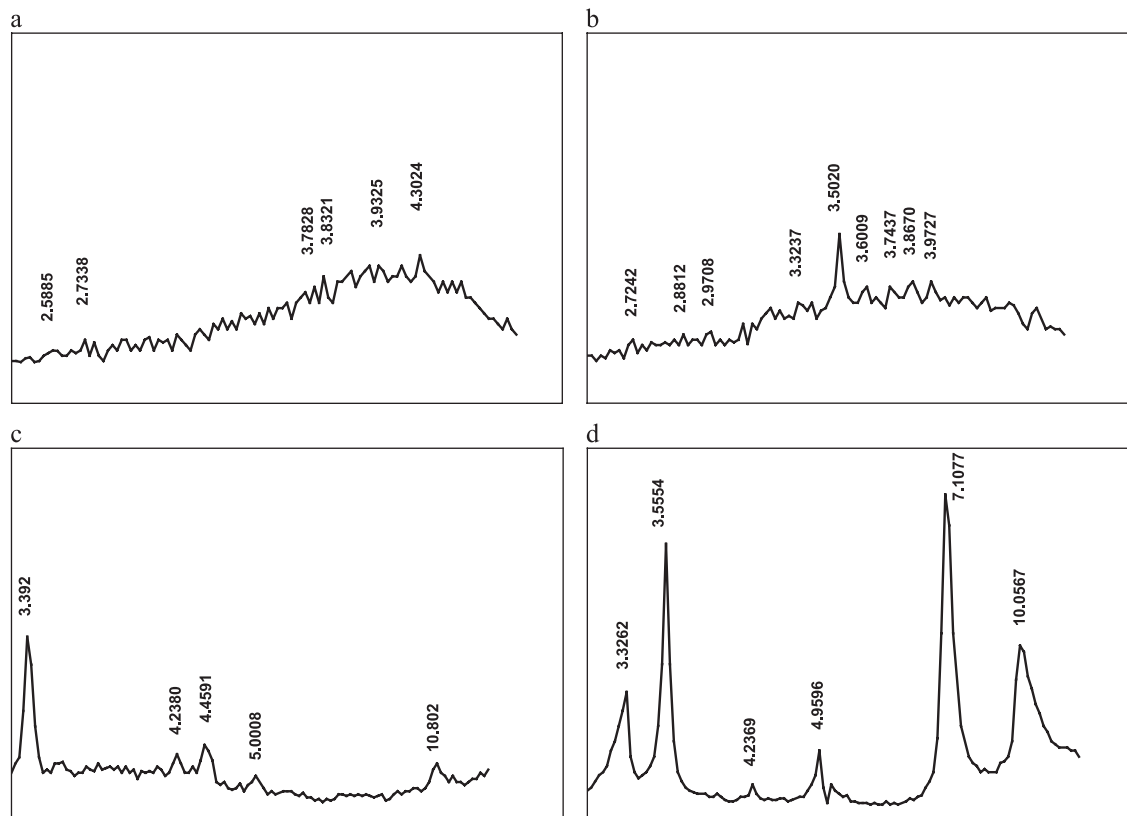


Fig. 2. (a) XRD pattern of silica fume (SF). (b) XRD pattern of metakaolin (MK). (c) RD pattern of raw (untreated) oil sands fine tailings. (d) XRD pattern of calcined oil sands fine tailings (CFT).

beam molds of $25 \times 25 \times 285$ mm ($1 \times 1 \times 11.25$ in.) using an external vibration table. After the casting, the molds were covered with a plastic sheet. All hardened specimens were removed from the molds in 24 h, and stored inside a closed container. Specimens were kept inside the container all the time, except for expansion measurements. For repeatability purpose, three specimens were prepared and tested for each mix. The average values of three test specimens are reported.

3. Results

3.1. Properties of SF, MK, and CFT

From Table 1, typical oxide analyses show that the content of acidic oxides (silica and alumina) varies widely

from one pozzolan to another, but it is evident that silica is a major constituent. The composition of SF is dominated by silica oxide (SiO_2). As for MK and CFT, their compositions are comparable, except that CFT contains about 10–15% of other metallic oxides and its alumina is significantly lower. The major component in Portland cement is calcium oxide.

Table 1 shows that CFT has the largest specific surface, followed by SF and MK. The large specific surface of CFT could increase its consumption of air entraining agent, but improve its pozzolanic reactivity. It might also decrease workability of the freshly mixed concrete.

To quantify why CFT has such a high specific surface, scanning electron microscope (SEM) and X-ray diffraction (XRD) analyses were conducted on the pozzolan samples. In the SEM photo, SF particles were spherical and small (less than 200 nm), resulting in a large specific surface (Fig. 1a). SEM photos (Fig. 1b) show that particles of MK

Table 3
Properties of freshly mixed concrete

	Control (PC)	7.5% SF	7.5% MK	7.5% CFT
Slump test, mm (ASTM C134)	200	160	180	120
Air content, % (ASTM C231)	5.8	5.6	6.2	5.9
Unit weight, kg/m^3 (ASTM C138)	2324.8	2328.6	2325.3	2321.4

Table 4
Development of compressive strength of concrete mixes (ASTM C39)

Mixes	Compressive strength (MPa)				
	3 days	7 days	14 days	28 days	90 days
Control	27	52	59	63	79
7.5% SF	32	55	63	68	91
7.5% MK	36	65	72	75	92
7.5% CFT	34	59	62	70	85

Table 5
Mechanical properties of concrete mixes (ASTM C78 and C469)

Mixes	Modulus of rupture (MPa)	Modulus of elasticity (MPa)
Control	9.8	27.8
7.5% SF	12.8	28.4
7.5% MK	10.4	31.2
7.5% CFT	10.2	30.9

preserved the layered structure of the original kaolinite particles. XRD patterns (Fig. 2a and b) show that the atomic regularity was probably destroyed or broken down by high-temperature calcination, the temperature of which is lower than that required for complete melting with production of glass on cooling. Fig. 2a and b, respectively, for SF and MK, only shows an amorphous halo, which is between 2.8 and 5.8 Å. There were no major peaks to indicate the presence of crystalline forms of silica and kaolin minerals, although a small peak at 3.5 Å on the diffraction pattern of MK indicates that some crystallinity was retained; the spacing corresponds approximately to a second-order basal reflection from kaolin. The XRD pattern of the raw tailings product (Fig. 2c) reveals the presence of illite, kaolin, and quartz which correspond to the 10 Å, 7 Å, and 3.3 Å peaks in the figure, respectively. The XRD patterns of CFT sample only show illite peaks and strong quartz peaks (Fig. 2d). While the principal kaolinite basal reflections at about 7 and 3.5 Å had vanished, a peak had appeared at about 4.4 Å, possibly attributable to a (02-) reflection in disordered kaolinite (1 Md). The illite appeared in the SEM photo (Fig. 1d) as irregular planar particles. Illite itself has a large specific surface, hence, the same property is reflected in the CFT. These SEM photos and XRD patterns explain why the specific surface in silica fume and the calcined fine tailings are large as compared with that in metakaolin. In addition, the specific surface becomes larger with finer particles.

3.2. Properties of freshly mixed concrete mixes

Slump, air content, and unit weight values for the four concrete mixes are given in Table 3. Slump values for the various mixes demonstrate that the reduction in workability due to a replacement of 7.5% by mass of cement with CFT was more pronounced as compared with those obtained by an equal amount of SF and MK replacement. This may also be interpreted as that, to obtain a given workability, CFT

Table 6
Length change of hardened concrete (ASTM C157)

	Moist curing (mm/mm)	Air curing (mm/mm)
Control	0.0081	− 0.0612
7.5% SF	0.00667	− 0.0187
7.5% MK	0.0047	− 0.0303
7.5% CFT	0.00133	− 0.0330

¹ positive indicate a gain in length.

Table 7
Resistance of concrete to rapid freezing and thawing (ASTM C666)

	Total mass lost (g)	Length changes ^a (%)	Relative dynamic modulus (%)	Durability factor ^b (%)
Control	7.2	0.0183	85.4	85.4
7.5% SF	4.1	0.0047	110.4	110.4
7.5% MK	4.2	0.0082	108.2	108.2
7.5% CFT	6.5	0.0123	94.3	94.3

^a Positive indicate a gain in length.

^b The durability factors are equal to the relative dynamic modulus because the specimens were cycled for the full 300 cycles. If the modulus fell below 60%, then the durability factor would differ.

concrete requires a greater quantity of superplasticizer than that for SF and MK. This may be attributed to the large specific surface of CFT.

Four concrete mixes yielded air content values in a comparable range between 5.6% and 6.2%, despite the large difference in specific surface among the pozzolans. The slight difference in air content in each mix should not significantly affect concrete strength and resistance to freeze–thaw.

3.3. Properties of hardened concrete mixes

3.3.1. Compressive strength development

The results of compressive strength tests at various ages are shown in Table 4. The control mix was designed to achieve a 28-day compressive strength of 60 MPa. The addition of any of the supplementary cementing materials did increase the strength of the concrete relative to that of the control mix. The rate of gain in strength at early ages was more rapid in MK and CFT concrete mixes than those in the control and SF mixes. At 28 days, the MK concrete displayed the highest strength (75 MPa), followed by CFT, SK, and the control mix. At 90 days, SF and MK attained comparable compressive strength. Table 4 indicates that the full potential of pozzolan supplements was developed over the long term rather than the short term.

3.3.2. Static modulus values of rupture and elasticity

Table 5 compares the static modulus values of rupture and elasticity obtained from tests complied with ASTM C78 and C469 for the control, SF, MK, and CFT concrete mixes. Marginal increases in modulus values of rupture and elasticity were observed with the addition of the supplementary

Table 8
Scaling resistance of concrete surfaces exposed to deicing chemicals (ASTM C672)

	Total mass lost (g)	Final rating
Control	5.1	3.33
7.5% SF	4.5	3.33
7.5% MK	2.5	2.87
7.5% CFT	4.2	3.00

Table 9
Average pore diameter of the blended cement pastes

Mix	Average pore diameter (Å)			
	3 days	7 days	14 days	28 days
Control (cement)	123.76	122.08	129.24	124.58
7.5% SF	98.42	87.06	86.20	83.46
7.5% MK	96.70	82.62	80.00	84.94
7.5% CFT	110.76	103.76	100.16	97.32

pozzolan. Again, the performances of SK and MK concrete mixes are comparable, while the CFT is slightly inferior.

3.3.3. Length change of hardened concrete (dry shrinkage)

Tests on length change of cured concrete specimens allow an examination of the capacity of the admixtures to control shrinkage under different conditions. Table 6 summarizes the results for moist and air curing at 28 days. All four concrete mixes exhibited an expansion under moist curing, and a shrinkage under air curing. However, all displayed expected and acceptable levels of performance.

3.3.4. Resistance to freeze–thaw and deicing

Tests were performed to investigate the resistance of air-entrained concrete to rapid freezing and thawing in the control, SF, MK, and CFT concrete mixes. The results are presented in Table 7. All the specimens showed only a small loss in mass and a small expansion after 300 cycles of freeze–thaw. Results from the relative dynamic modulus of elasticity showed that concrete containing 7.5% SF had the best resistance to freeze–thaw conditions after 300 cycles. It had the highest relative dynamic modulus and durability factor. All the other three supplementary pozzolans displayed high durability factors and had less than 0.02% length change, showing adequate performance under these conditions. The improved durability could be attributed to

the pore refinement produced by the pozzolanic reaction. All the other three mixes (the control, MK, and CFT) performed well overall in the freeze–thaw test, as the values of the durability factors were well over the required 60% mark.

The scaling resistances of MK, SF, and CFT concrete exposed to deicing chemicals were also studied, and their test results are summarized in Table 8. SF, MK, and CFT had 3.33, 2.87, and 3.00 ratings of the surface conditions after 50 cycles of freeze–thaw, respectively. SF and CFT concrete both performed well with respect to the mass lost in each specimen, but MK was superior, displaying almost half the mass lost by the SF specimen.

3.3.5. Rapid chloride permeability

Rapid chloride permeability tests were conducted on concrete specimens at 28 days. This chloride permeability test method consisted of monitoring the amount of electrical current that passed through 51-mm (2 in.) thick cores during a 6-h period. A potential of 60 V dc was maintained across the ends of the specimens, one of which was immersed in 3.0% sodium chloride solution, the other in a 0.3 N sodium hydroxide solution. The quantities of electric charges passing through the concrete samples were 996, 229, 195, and 799 C for the control, SF, MK and CFT specimens, respectively (according to ASTM C1202, the chloride ion penetrability is classified as very low when charges passed are in a range of 100–1000 C). The higher the electric current passing through the specimen, the less the resistance of the specimen to chloride ion penetration or the more porous the specimen is. The measured results indicate that the addition of supplementary pozzolan reduced the pore sizes, thus lowering the permeability. MK was the most effective supplementary pozzolan in reducing the permeability, followed by SF. The permeability reduction ob-

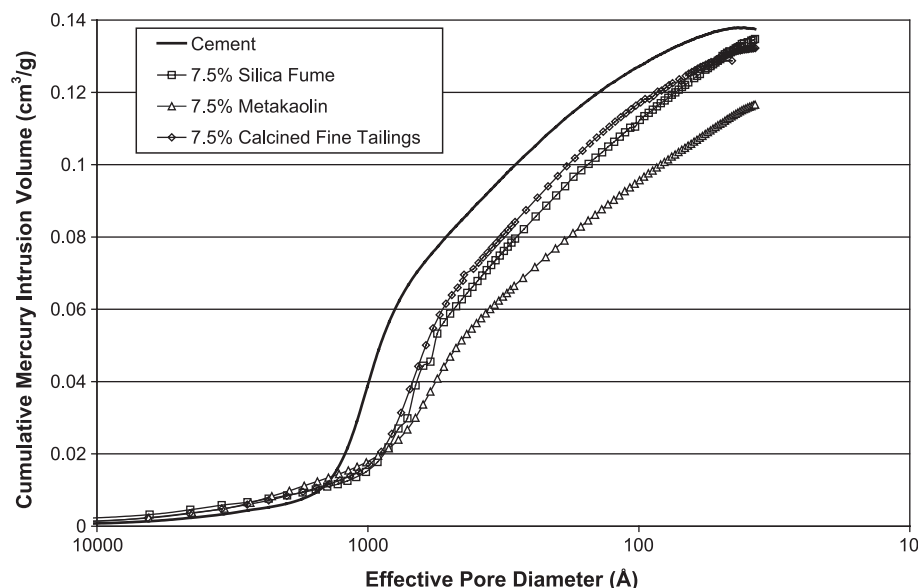


Fig. 3. Pore size distribution for various blended cement pastes at 7 days.

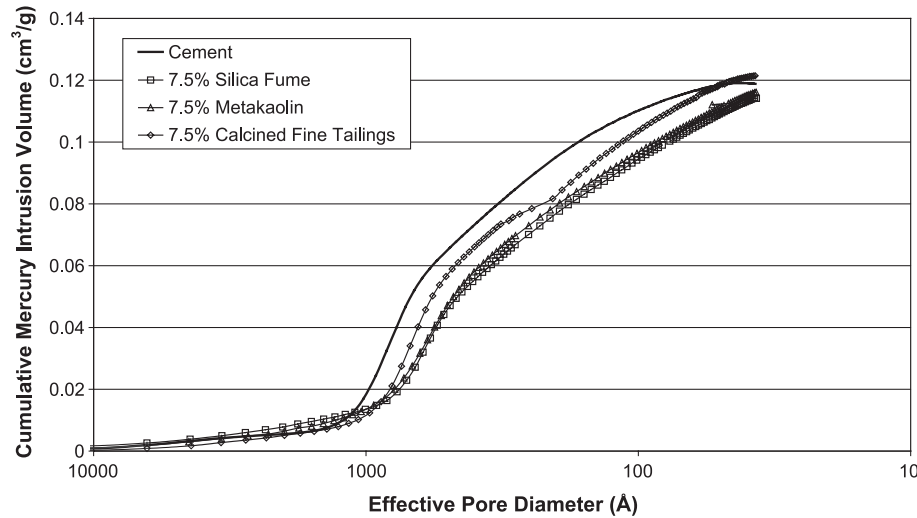


Fig. 4. Pore size distribution for various blended cement pastes at 28 days.

served in CFT specimens was marginal as compared with the control.

3.4. Pozzolanic reaction of SF, MK, and CFT in blended cement pastes

3.4.1. Average pore size and pore size distribution of blended cement pastes

Table 9 is a summary of development of the average pore size in the control, SF, MK, and CFT cement pastes obtained from the mercury intrusion porosimetry tests. The control paste containing no supplementary cementing material had the largest average pore size. In addition, there was no pore size reduction in the control paste during the curing period. However, the supplementary cementing materials in the cement pastes reduced the average size of the pore diameter. The most effective pozzolan supplement in reducing the pore size was MK, while the smallest effect in decreasing the pore size was observed in the cement paste containing 7.5% calcined tailings. Figs. 3 and 4 compare the pore size distributions of the four blended cement pastes at 7 and 28 days, respectively. There was no substantial change in pore sizes between 7 and 28 days, implying that most of the pozzolanic reactions in the pastes occurred in the early stage. The pore size reduction effects observed in the blended cement pastes are consistent with those measured in the rapid chloride permeability tests. MK concrete, with the smallest average pore diameter, provided the highest

resistance to the electrical current passed through the specimen, followed by SF, CFT, and the control concrete.

3.4.2. Ca(OH)_2 content of blended cement pastes

Table 10 shows that by using supplementary pozzolans in the cement paste, Ca(OH)_2 content produced from the hydration of cement paste was reduced. MK was very effective in reducing the amount of Ca(OH)_2 initially, but became less effective after 14 days. This could explain its effect on early strength development. SF is shown to be rather less effective at the beginning of curing. However, after 14 days of moist curing, the Ca(OH)_2 content of the SF pastes quickly declined to the same level as the MK paste. It is interesting to note that among the three supplementary pozzolans CFT had the highest content of Ca(OH)_2 , even though its chemical composition is quite similar with that of MK (Table 1). The low activities could be caused by the significant levels of nonkaolin minerals, particularly illite (Fig. 2c).

3.5. Alkali–silica reaction

ASR occurs when the alkalis in the cement react with certain forms of silica found in the aggregate, forming an alkali–silica gel. This gel has a strong affinity for water and has a tendency to swell, causing cracking in the paste matrix

Table 10
 Ca(OH)_2 content in the different blended cement pastes

Mixes	Ca(OH)_2 content (%)			
	3 days	7 days	14 days	28 days
Control (cement)	14.31	14.56	15.21	17.07
7.5% SF	11.18	10.12	8.76	10.53
7.5% MK	10.44	9.17	8.92	10.40
7.5% CFT	11.27	10.32	11.18	12.71

Table 11
Alkali–silica reaction in mortar mixes (ASTM C441)

Mixes	Expansion (%)			
	14 days	28 days	60 days	15 months
Control (high-alkali cement)	0.326	0.452	0.480	0.486
Portland cement	0.182	0.231	0.253	0.257
7.5% SF	0.071	0.156	0.168	0.254
7.5% MK	0.069	0.147	0.168	0.220
7.5% CFT	0.160	0.321	0.346	0.371

and deterioration of the concrete. Mortar bars containing a highly reactive aggregate (Pyrex-Borosilicate glass) were used to compare the effectiveness of SF, MK, and CFT in controlling ASR over time, and the test results are shown in Table 11. After 14 days, the control mix with the high-alkali cement displayed the largest elongation, followed by the PC, CFT, SF, and MK. Most of the expansion occurred during the early period, and started to level off at 28 days. However, at 28 days and beyond, the order for greatest elongation was high-alkali cement, CFT, PC, SF, and MK. It was observed that the cracks and surface deteriorations present in the control and Portland cement specimens were significantly reduced when any one of the supplementary pozzolans was used.

4. Concluding remarks

The aim of this research study is to investigate the potential use of calcined oil sands fine tailings (CFT) as a supplementary cementing material for concrete. A series of tests were conducted on concrete mixes, blended cement pastes, and cement mortar to compare the performance of CFT with those of SF and MK. The current research presented in this paper has demonstrated that CFT is suitable as a partial replacement for Portland cement, improving compressive and flexural strengths in both the short and the long term. The altered pore structure provided by CFT to the cement paste, mortar, or concrete, has been demonstrated to improve resistance to aggressive deicing chemicals, freeze–thaw conditions, and chloride penetration. CFT was also effective in preventing excessive expansion of concrete due to ASR. However, CFT is currently still in its infancy and at a disadvantage in research terms because it does not offer performance enhancement above and beyond existing products such as SF and MK. However, CFT could be marketed as a low-cost option to cement-production-related environmental issues, while providing some of the benefits of MK. To improve the performance of CFT in concrete, further research in several areas are required. They include the

following: effects of calcination temperature and grinding on its pozzolanic properties, sulfate resistance, strength at elevated temperatures to ensure that the reaction products are similar to MK, and the effects of other mineral products (or impurities) in CFT on long-term properties of concrete.

Acknowledgements

This research work was proposed by George Jones and Ted Lord of Syncrude Canada, and their ongoing encouragement and input is appreciated. Financial support from Syncrude and ECCI is gratefully acknowledged. Part of the experimental work was conducted by Terry Quinn, Jaye Moore, and Monique Castonguay. Constructive comments from reviewers are appreciated.

References

- [1] N.R. Morgenstern, A.E. Fair, E.C. McRoberts, Geotechnical engineering beyond soil mechanics—a case study, *Can. Geotech. J.* 25 (1988) 50–55.
- [2] M.A. Caldarone, K.A. Gruber, R.G. Burg, High reactivity metakaolin: a new generation mineral admixture, *Concr. Int.*, (November 1994) 37–40.
- [3] J.M. Khatib, S. Wild, Pore size distribution of metakaolin paste, *Cem. Concr. Res.* 26 (1996) 1545–1553.
- [4] S. Wild, J.M. Khatib, A. Jones, Relative strength, pozzolanic activity and cement hydration in superplasticized metakaolin concrete, *Cem. Concr. Res.* 26 (1996) 1537–1544.
- [5] S. Wild, J.M. Khatib, Portlandite consumption in metakaolin cement pastes and mortars, *Cem. Concr. Res.* 27 (1997) 137–146.
- [6] B.B. Sabir, S. Wild, J. Bai, Metakaolin and calcined clays as pozzolans of concrete: a review, *Cem. Concr. Compos.* 23 (2001) 441–454.
- [7] C.S. Poon, L. Lam, S.C. Kou, Y.L. Wong, R.C.K. Wong, Rate of pozzolanic reaction of metakaolin in blended cement pastes, *Cem. Concr. Res.* 31 (2001) 1301–1306.
- [8] L. Day, B.K. Marsh, Measurement of porosity in blended cement pastes, *Cem. Concr. Res.* 18 (1998) 63–73.
- [9] H.F.W. Taylor, *Cement Chemistry*, Academic Press, London, 1990, pp. 261–263.